Environ. Sci. Technol. **2010,** *44,* 9578–9583

Microbial Electrodialysis Cell for Simultaneous Water Desalination and Hydrogen Gas Production

MAHA MEHANNA, PATRICK D. KIELY, DOUGLAS F. CALL, AND BRUCE. E. LOGAN*

Department of Civil and Environmental Engineering, The Pennsylvania State University, University Park, Pennsylvania 16802, United States

Received July 28, 2010. Revised manuscript received October 22, 2010. Accepted November 1, 2010.

A new approach to water desalination is to use exoelectrogenic bacteria to generate electrical power from the biodegradation of organic matter, moving charged ions from a middle chamber between two membranes in a type of microbial fuel cell called a microbial desalination cell. Desalination efficiency using this approach is limited by the voltage produced by the bacteria. Here we examine an alternative strategy based on boosting the voltage produced by the bacteria to achieve hydrogen gas evolution from the cathode using a three-chambered system we refer to as a microbial electrodialysis cell (MEDC). We examined the use of the MEDC process using two different initial NaCl concentrations of 5 g/L and 20 g/L. Conductivity in the desalination chamber was reduced by up to 68 $\pm$ 3% in a single fed-batch cycle, with electrical energy efficiencies reaching 231 $\pm$ 59%, and maximum hydrogen production rates of 0.16 $\pm$ 0.05 m^3 H_2/m^3 d obtained at an applied voltage of 0.55 V. The advantage of this system compared to a microbial fuel cell approach is that the potentials between the electrodes can be better controlled, and the hydrogen gas that is produced can be used to recover energy to make the desalination process self-sustaining with respect to electrical power requirements.

Introduction

The use of desalination for the production of drinking water is increasing worldwide, and the energy needs for this process are a major concern (*1*). Of the different commercially available technologies, reverse osmosis (RO) is the least energy intensive process, but it still requires ~3.7 kWh/m^3 (*2*). RO energy requirements can be reduced through alternation of the chemical species in the feedwater through ion exchange (*3*) or by reducing the salt concentration of the feedwater. It was recently discovered that a new type of bioelectrochemical system (*4, 5*), called a microbial desalination cell (MDC), could be used to partially or completely desalinate water while at the same time generating electrical power (*6*–*8*).

An MDC has three chambers separated by two membranes, with the salt water to be desalinated contained in the middle chamber. Bacteria grow on the anode and oxidize organic matter and release electrons to the anode and protons into solution. Charge is balanced in the anode chamber through the transfer of negatively charged (chloride) ions from the middle chamber through an anion exchange membrane (AEM) into the anode chamber. At the cathode, protons removed through reduction of oxygen are replaced by cations (sodium) transferred through a cation exchange membrane (CEM) separating the middle and cathode chamber. The process is similar to water electrodialysis, except that no external power source is needed for an MDC. Domestic wastewater, which has a low conductivity (~1 mS/cm), has been proposed as a source of organic matter for the anode chamber. In this case, power generation and desalination in the MDC are increased due to the entropic energy difference between the anode and desalination chambers due to their salinity differences, in a manner similar to that used for power generation using reverse electrodialysis (RED). It was previously demonstrated using an MDC with three equally sized chambers that it was possible to achieve up to 63% desalination of the water in the middle chamber, while generating a maximum power density of 480 mW/m^2 in a single fed-batch cycle (*7*).

One limitation of the MDC approach as it has been used so far is that the voltage is not constant over the cycle. In a fed-batch process, the maximum power is achieved at the beginning of a cycle when the salinity difference is the greatest, and the concentration of organic matter is highest in the anode chamber. Over time, the voltage decreases and the osmotic pressure is reduced between the anode and desalination chamber. In addition, the maximum voltage that can be achieved between the electrodes is limited to that produced by the bacteria on the anode and oxygen reduction at the cathode. An alternative approach that is proposed here is to boost the voltage produced by the bacteria using a power source and not use oxygen at the cathode. This will result in hydrogen production at the cathode, as previously shown using microbial electrolysis cells (*9*). This new device, which we call a microbial electrodialysis cell (MEDC), could therefore achieve water desalination while at the same time producing hydrogen gas that could be used as a fuel. Part of the hydrogen gas could be used for the MEDC process, with excess hydrogen available to help power a downstream RO process. Performance of the MEDC was evaluated here in terms of the conductivity decrease in the desalination chamber, hydrogen recovery, hydrogen production rate, and energy recovery (electrical and overall energy).

Materials and Methods

MEDC Construction. The MEDC was constructed as previously described (*7*) from three cubes of polycarbonate drilled to contain a cylindrical chamber 3 cm in diameter, except that the volume of the cathode chamber was increased to 27 mL in order to attach a gas collection tube (1.6 cm inner diameter, 7 cm long) to the top of the reactor (*10*) (Figure S1, Supporting Information). The anodic and the desalination chambers were each 2 cm long (14 mL each). The desalination chamber was separated from the anode chamber by an AEM (AMI-7001) and from the cathode chamber by a CEM (CMI-7000; both from Membranes International Inc.). The resistivities of the membranes were <6.5 Ω m (CEM) and <8.7 Ω m (AEM), and the total exchange capacities were 1.3 meq/g (CEM) and 1.0 meq/g (AEM). Both membranes had the same thickness (0.46 mm). All membranes were preconditioned by immersion in a 0.5 M NaCl solution overnight and rinsing in distilled water.

The anodes were carbon cloth (type A; E-TEK) heat-treated at 450 °C for 30 min. Cathodes were made by applying

* Corresponding author phone: (814)863-7908; e-mail: blogan@psu.edu.

10.1021/es1025646
Published on Web 11/15/2010

platinum (0.5 mg/cm^2) and four diffusion layers on a 30% wet-proofed carbon cloth (type B-1B; E-TEK) (*11*). Both electrodes had a projected surface area of 7 cm^2.

Microorganisms and Medium. The anodes were preacclimated (enriched with a biofilm) for 40 days in microbial desalination cells (MDCs) (*7*) (Figure S2, Supporting Information). Preacclimation of the anodic bacterial population to chloride was needed because a series of preliminary MEDC experiments done with anodes inoculated directly with wastewater or first acclimated in MFCs did not produce current. The medium used for the MEDC anodes contained a 50 mM phosphate buffer solution (PBS; 4.58 g/L Na_2HPO_4, 2.45 g/L NaH_2PO_4•H_2O, 0.31 g/L NH_4Cl, 0.13 g/L KCl), sodium acetate (2 g/L), and mineral (12.5 mL) and vitamin (5 mL) solutions (*12, 13*). The desalination chamber contained 5 g/L or 20 g/L NaCl in distilled water. The cathode contained 50 mM PBS buffer.

Operation. Initial tests conducted at different applied voltages (E_{ap}) by a power source (model 3645A; Circuit Specialists, Inc.) showed that 0.55 V provided stable and improved performance compared to three other voltages (0.9 V, 0.65 V, and 0.45 V; data not shown); therefore, only E_{ap} = 0.55 V was examined in detail here. Measurements of the anodic and the cathodic potentials versus reference electrodes also showed that when 0.55 V was applied the anode potential was similar to that produced in MDCs (with no applied voltage) where the anodes were preacclimated. Current was determined by measuring the voltage across a 10 Ω resistor connected in series with the power supply using a multimeter (model 2700; Keithley Instruments, Inc.). Anode and cathode potentials were continuously recorded using Ag/AgCl reference electrodes (RE-5B; BASi; + 206 mV vs a standard hydrogen electrode, SHE) placed in the anode and cathode chambers. All voltages are reported here versus SHE. After each cycle, the reactors were drained and refilled with substrate solution, and all three compartments were sparged with ultra high purity nitrogen gas for 15 min. Experiments were repeated twice and run in duplicate in a 30 °C constant temperature room. A cycle was considered complete when the gas production reached a plateau.

Analyses. Continuous gas production was measured using a respirometer (AER-200; Challenge Technology). Gas from the respirometer was collected in sampling bags (250 mL capacity, Cali-5 bond; Calibrated Instruments Inc.) and analyzed using gas chromatography as previously described (*14*).

Sodium and chloride ion concentrations were measured using combination electrodes and a meter (SympHony SB90M5; VWR International). Phosphate was measured using the total phosphate method (HACH Company, Loveland, CO). Acetate was analyzed using a gas chromatograph (Agilent, 6890) equipped with a flame ionization detector and a fused silica capillary column (Agilent, DB-FFAP) with helium as carrier gas. Solution pH was monitored using a pH probe and meter (SympHony SB70P; VWR International). Electrolyte solution conductivities per cm were measured using a conductivity electrode (2 Cell Epoxy; SympHony SB90M5 m; VWR International). All measurements were done at the beginning and end of each fed-batch cycle. Chemical oxygen demand (COD) was measured according to standard methods (TNTPlus COD Reagant; HACH Company) (*15*).

Electromotive Force. The electromotive force (E_{emf}) generated by the diffusion of sodium and chloride ions across the membranes is the sum of the potentials generated by the diffusion of Cl^- (E_{AEM}) across the AEM and Na^+ across the CEM (E_{CEM})

$$E_{emf} = E_{AEM} + E_{CEM} \quad (1)$$

E_{emf} was calculated as described previously (*7, 16*).

Hydrogen Recovery and Production. MEDC performance was evaluated in terms of Coulombic efficiency (C_E), cathodic hydrogen recoveries (r_{cat}), electrical energy efficiency (η_E), overall energy recovery based on both substrate and electrical energy (η_{E+S}), and maximum volumetric hydrogen production rate (Q_{max}) as previously described for MECs (*10, 17*). The current (I; A/m^2) was normalized to the surface of the anode (0.0007 m^2).

Bacterial Community and Phylogenetic Analysis. Genomic DNA extracted from the anode biofilm using a PowerSoil DNA isolation kit (MO BIO Laboratories), gene cloning, and 16S rRNA gene sequencing for community analysis were conducted as previously described (*18*). Extracted DNA was amplified by PCR using the universal 16S rRNA bacterial primers 530F (5′-GTCCCAGCMGCCGCGG-3′) and 1490R (5′-GGTTACCTTGTTACGACTT-3′) (*19*). Replicate PCR products were purified, ligated, and cloned using a TOPO TA cloning kit (Invitrogen). Plasmids were extracted (E-Z 96 Fastfilter Plasmid Kit) and sequenced (M13R primer, ABI 3730XL DNA sequencer, Applied Biosystems). Sequences were identified by comparing them to the nucleotide collection (nr/nt) of the National Center for Biotechnology Information (www.ncbi.nlm.nih.gov/ BLAST/) with the BLASTn algorithm.

16S rRNA fragments of clones representing distinct phylotypes (>97% similarity) were plotted against the total number of clones. Sampling coverage was calculated as previously described (*20*), with rarefaction curves used to confirm that sufficient representatives had been sequenced (*21*) (Figure S3, Supporting Information) .

Fluorescent in Situ Hybridization. For each reactor, identical sized sections of the anode were cut off, fixed in tubes containing 4% paraformaldehyde, and vortexed with sterile glass beads. The supernatant was filtered onto 0.2 μm black polycarbonate filters (*23*). The filters were then cut, placed in sterile 200 μL PCR tubes, and hybridized (*23*). A species specific probe for *Geobacter sulfurreducens* (GEO2) was labeled with Alexa Fluor 594 (Invitrogen) along with two helper probes (HGEO2-1 and HGEO2-2) (probe concentrations of 10 ng/μL) (*24, 25*). Hybridized samples were placed onto slides and counterstained using 4°,6-diamidino-2-phenylindole (DAPI) (SlowFade Gold, Invitrogen). Manual cell counts were made on 15 equally sized grids placed at random over five separate captured images taken at 1000× using an Olympus BX61 epifluorescent microscope, with images recorded using a DP72 digital camera. Controls were included to check for autofluorescence (no probe) and nonspecific binding of the dye (nonsense probe).

Results and Discussion

Desalination Performance. The conductivity of the water in the desalination chamber decreased by 68 ± 3% for the 5 g/L NaCl sample and by 37 ± 4% for the 20 g/L NaCl sample by the end of a single batch-fed cycle (Figure 1). Control experiments were performed under the same conditions using sterile media to determine changes that would result from differences in osmotic pressure across the membranes under an applied voltage of 0.55 V during the same period of time as the biotic experiments. In these control experiments the conductivity in the desalination chamber decreased by 22 ± 2% (5 g/L NaCl) and 31 ± 2% (20 g/L) due to dialysis (data not shown). Therefore, in the absence of current generation by bacteria there was slightly greater desalination of the 20 g/L salt solution than the 5 g/L solution due to the larger osmotic pressure differences. Biotic current generation resulted in substantially improved desalination of the 5 g/L solution. In the case of the 20 g/L, it is likely that the increase in chloride concentration in the anode chamber adversely affected current generation by the bacteria. All three compartments were tested for acetate and phosphate at the end

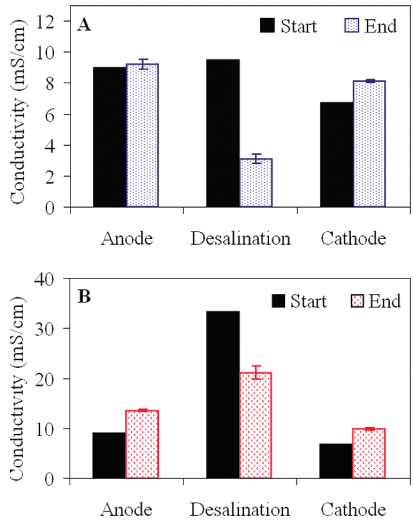

FIGURE 1. Conductivities in MEDC chambers with (A) 5 g/L and (B) 20 g/L NaCl in the desalination chamber.

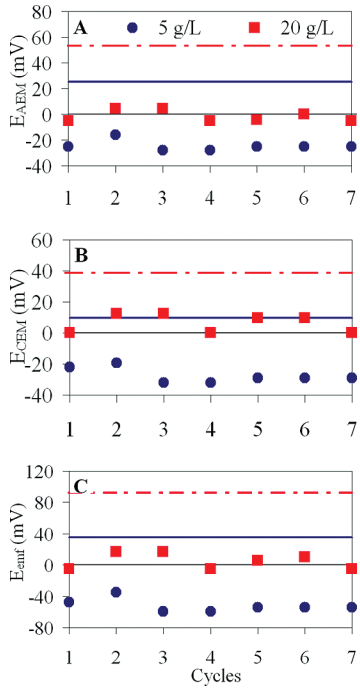

FIGURE 2. Membrane potentials generated by ion concentration gradients: (A) across the AEM from the desalination chamber toward the anode chamber; (B) across the CEM, from the desalination chamber to the cathode chamber; and (C) the generated electromotive force (EMF). The lines indicate potentials at the beginning of each cycle. The solid symbols indicate potentials recorded at the end of the batch cycles.

of every cycle. There was no evidence of acetate or phosphate migration into the desalination chamber.

Membrane Electromotive Force. The magnitude of the membrane electromotive force over successive cycles provides insight into the extent of charge transfer relative to equilibrium. The potentials E_{AEM} and E_{CEM} at the beginning of each cycle relative to movement of ions from the middle chamber into the electrode chambers were both highly positive, resulting in an overall positive E_{emf} (Figure 2). The best desalination performance was obtained when the E_{emf} was negative, indicating that the ionic concentration in the center chamber was driven past the equilibrium point, achieving lower ionic strength concentrations in the desalination chamber than the anode or cathode compartments. The E_{emf} obtained with 5 g/L NaCl was negative, while it was positive with the 20 g/L NaCl, consistent with a larger relative decrease in solution conductivity with 5 g/L than 20 g/L NaCl. The lack of a negative E_{emf} for the 20 g/L case further suggests that desalination was primarily limited by the activity of the bacteria on the anode at higher salt concentrations.

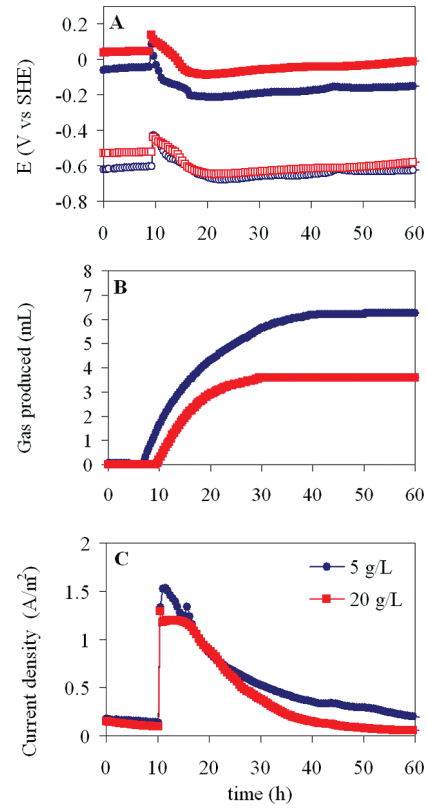

FIGURE 3. Example of (A) anode (filled symbols) and cathode (open symbols) potentials, (B) gas production, and (C) current densities over a fed-batch cycle second of seven cycles used to calculate data shown in Table S1, Supporting Information.

Electrode Potentials. The cathode potentials were similar for both salt concentrations, but the anode potentials were more negative with 5 g/L NaCl (Figure 3A). This result confirms that the improved desalination and hydrogen recoveries obtained with 5 g/L NaCl were due to the lower initial concentration of salt and thus a lower final concentration of Cl^- in the anode chamber. High Cl^- concentrations can inhibit bacterial growth. Chloride concentrations in the anodic compartment were measured at the end of each batch cycle (Figure S4, Supporting Information). Less chloride was found in the anodic compartment with the MEDC containing 5 g/L compared to the one with 20 g/L.

Hydrogen Production. After more than 25 days of operation, the gas that was produced was 100% hydrogen with no methane detected. Over one batch cycle, the MEDC with 5 g/L NaCl produced 6.5 ± 1.4 mL of hydrogen and the one with 20 g/L generated 2.7 ± 1.0 mL (Figure 3B). Higher hydrogen recoveries were obtained with the lower salt concentration (5 g/L). These results were in accordance with the results shown above regarding improved performance of the MEDC operated with a lower salt concentration.

Coulombic efficiencies, or the recovery of electrons from the utilized substrate, were 48 ± 4% with 5 g/L NaCl (38 ± 3% COD removal) and 16 ± 2% with 20 g/L (54 ± 5% COD removal) (Table S1, Supporting Information). The cathodic hydrogen recovery, defined as the fraction of electrons reaching the cathode that are recovered as hydrogen gas, reached r_{cat} = 92 ± 19% with 5 g/L NaCl and 97 ± 40% with

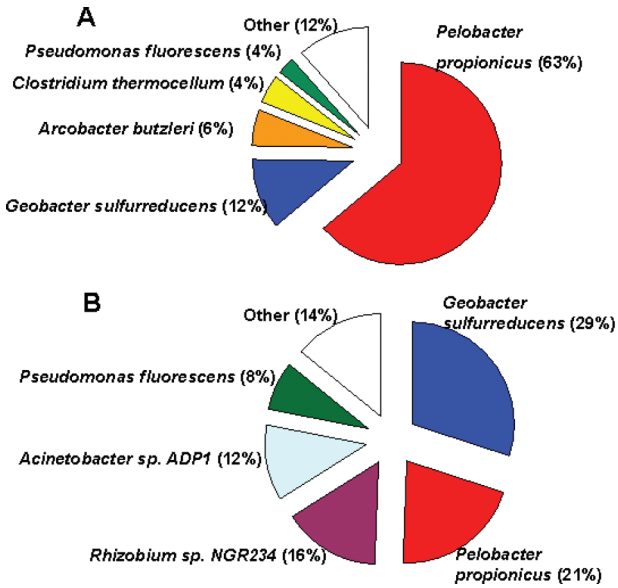

FIGURE 4. Bacterial 16S rRNA community analysis of anode biofilm in a microbial electrodialysis cell supplied (A) 5 g/L and (B) 20 g/L NaCl.

20 g/L. The overall hydrogen recoveries in the MEDCs were $r_{H2} = 44 \pm 10\%$ (5 g/L) and $15 \pm 4\%$ (20 g/L). These r_{H2} values are lower than those previously reported of 91% at $E_{ap} = 0.6$ V (*26*) using acetate in a two-chamber MEC with an anion exchange membrane.

The maximum volumetric hydrogen production rates were $Q_{max} = 0.11 \pm 0.09$ m^3 H_2/m^3 d with (5 g/L NaCl) and 0.16 ± 0.05 m^3 H_2/m^3 d (20 g/L). These hydrogen production rates are lower than those obtained in MECs using anion or cation exchange membranes at similar applied voltages ($Q_{max} = 0.3 - 1.1$ m^3 H_2/m^3 d at $E_{ap} = 0.45 - 0.6$ V) (*9, 26, 27*). The design of the system here, which has relatively large electrode spacing due to the middle chamber, can increase internal resistance and result in pH gradients across the membranes, both of which are known to reduce MEC performance (*28, 29*). At the end of the cycles, the pH values were 5.2 ± 0.1 in the anodic compartment, 6.3 ± 0.2 in the desalination chamber, and 9.4 ± 0.7 in the cathodic compartment for 5 g/L cycles. Previous studies of MECs using membranes revealed that a large part of potential losses in the system were associated with a pH gradient across the membrane.

Energy Recovery. The energy efficiencies obtained in the MEDCs reached $\eta_E = 231 \pm 59\%$ (5 g/L NaCl) and $213 \pm 38\%$ (20 g/L NaCl), suggesting that sufficient hydrogen was produced to power the MEDC. These values are comparable to those achieved for MECs using membranes at similar applied voltages ($\eta_E = 169-261\%$ at $E_{ap} = 0.5-0.6$ V) (*9, 26, 27*). The relatively high values of η_E are due to the low current densities output. The current densities were 1.4 ± 0.2 A/m^2 with 5 g/L of NaCl and 1.2 ± 0.2 A/m^2 with 20 g/L NaCl (Figure 3C).

Community Analysis of MEDCs Anodic Microbial Populations. 16S rRNA clone library analysis identified both anode biofilms to be dominated by clones with significant similarity (>97%) to members of the *Geobacteraceae* family. Clones showing significant similarity to *Pelobacter propionicus* represented 63% clones in the MEDC with 20 g/L NaCl and 21% with 5 g/L NaCl. *G. sulfurreducens* comprised a significant proportion of both microbial communities, representing 12% (5 g/L NaCl) and 29% (20 g/L NaCl) of the 16S rRNA clones (Figure 4). Clones with significant similarity (>97%) to *Rhizobium etli* CFN 42 and *Acinetobacter* sp. ADP1 represented 28% of the anode of the MEDC supplied 20 g/L NaCl but were not identified on anodes supplied 5 g/L.

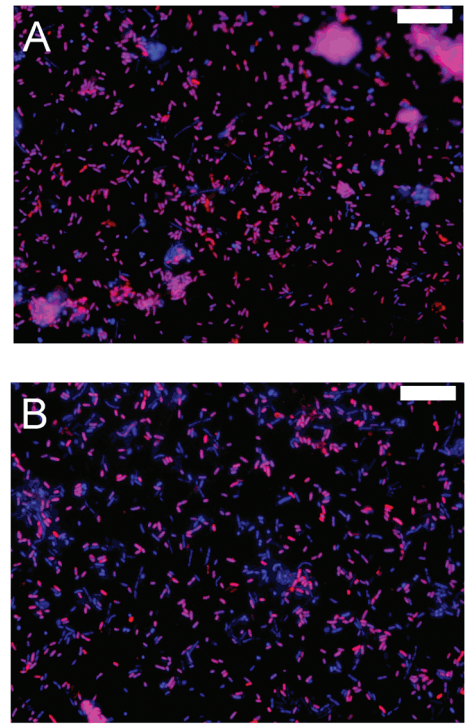

FIGURE 5. FISH images from MEDC anode biofilms operating with (A) 5 g/L and (B) 20 g/L NaCl showing *G. sulfurreducens* (pink/red) and all bacteria and Archaea (blue). White bars equal 10 μm.

Neither of these Gram (-) bacteria are expected to be associated with current generation. *Acinetobacter* species are ubiquitous, nonmotile microbes typically associated with nosocomial infections of immuno-compromised patients (*30*), and *R. etli* is commonly associated with nitrogen fixation and legumes (*31*).

Due to possible PCR bias associated with 16S rRNA clone libraries, verification of community profiles using FISH was carried out to quantify the relative numbers of *G. sulfurreducens*. FISH images (Figure 5) showed that electrode surfaces were covered by similar numbers of cells ($3.1 \times 10^7 \pm 6.0 \times 10^6$ cells/cm^2 for 5 g/L NaCl and $3.1 \times 10^7 \pm 4.0 \times 10^6$ cells/cm (*2*) for 20 g/L; anode projected surface area). FISH analysis confirmed the presence and predominance of *G. sulfurreducens* under both operating conditions, with a larger percentage ($79 \pm 4\%$) in the lower salinity condition than in the higher salinity case ($63 \pm 6\%$). *G. sulfurreducens* is typically identified as the dominant microbe in various BES when acetate is supplied as the substrate (*32*). Although this bacterium is capable of reducing iron in medium containing up to one-half the concentration of NaCl found in seawater (~18 g/L) (*33*), it is most commonly cultured and operated in BESs with salinities around 2 g/L (*33−35*). Furthermore, community analysis of marine sediment MFC anodes identified little to no *Geobacter* species (*36−38*), suggesting a preference of low salinities for this genera. The correlation of improved reactor performance with increased numbers of *Geobacteraceae* is not unexpected as *G. sulfurreducens* produces high current densities in MFCs (*39*) and MECs (*40*).

Outlook. MEDCs can be used to both desalinate water as well as produce hydrogen gas. The energy demand for the MDEC ranged between 2.2 (5 g/L NaCl) and 1.2 kWh/m^3 (20 g/L NaCl). However, more than twice this amount of energy was recovered in the hydrogen gas (η_E of 231% and 213%), suggesting that the produced hydrogen could be used to provide the power for the MDEC or additionally for other processes. The gas produced in the MEDC was 100% hydrogen, even after 25 days of operation. Avoiding methane

gas production has been challenging in single-chamber MECs (*41*−*43*), but this is much less of a problem with two-chamber MECs (*26, 28*) or the three-chambered system used here as the separating membrane keeps the hydrogen gas separated from the microbes in the anode chamber. The main advantage of a MDEC compared to a MDC may be that greater control of the process can be achieved by constant application of a voltage to the system. It was shown here that conductivity in the desalination chamber could be decreased by 68 ± 3%, compared to a maximum of 60 ± 7% in the MDC (*7*). The extent of desalination could possibly be further improved by varying the voltage added to the system, particularly at the end of the cycle when the anode potential becomes more positive and the desalination chamber conductivity is low. Examination of variable voltages and the development of continuous flow systems are needed to advance these new microbial desalination technologies.

Acknowledgments

This research was supported by Award KUS-I1-003-13 from the King Abdullah University of Science and Technology (KAUST), the National Science Foundation Graduate Research Fellowship (D.F.C.), and the National Water Research Institute Ronald B. Linsky Fellowship (D.F.C.).

Supporting Information Available

Four additional figures and one table. This material is available free of charge via the Internet at http://pubs.acs.org.

Literature Cited

(1) Christen, K. Environmental costs of desalination. *Environ. Sci. Technol.* **2007**, *41* (16), 5579–5579.
(2) Semiat, R. Energy Issues in Desalination Processes. *Environ. Sci. Technol.* **2008**, *42* (22), 8193–8201.
(3) Sarkar, S.; SenGupta, A. K. A new hybrid ion exchange-nanofiltration (HIX-NF) separation process for energy-efficient desalination: Process concept and laboratory evaluation. *J. Membr. Sci.* **2008**, *324* (1−2), 76–84.
(4) Logan, B. E. *Microbial fuel cells*; J. Wiley & Sons, Inc.: 2008.
(5) Rabaey, K.; Angenent, L.; Schroder, U.; Keller, J. *Bioelectrochemical Systems: From Extracellular Electron Transfer to Biotechnological Application*; IWA Publishing: 2009.
(6) Cao, X. X.; Huang, X.; Liang, P.; Xiao, K.; Zhou, Y. J.; Zhang, X. Y.; Logan, B. E. A new method for water desalination using microbial desalination cells. *Environ. Sci. Technol.* **2009**, *43* (18), 7148–7152.
(7) Mehanna, M.; Saito, T.; Yan, J.; Hickner, M.; Cao, X.; Huang, X.; Logan, B. E. Using microbial desalination cells to reduce water salinity prior to reverse osmosis. *Energy Environ. Sci.* **2010**, *3* (8), 1114–1120.
(8) Jacobson, K. S.; Drew, D. M.; He, Z. Efficient salt removal in a continuously operated upflow microbial desalination cell with an air cathode. *Bioresour. Technol.* **2011**, *102* (1), 376−380.
(9) Liu, H.; Grot, S.; Logan, B. E. Electrochemically assisted microbial production of hydrogen from acetate. *Environ. Sci. Technol.* **2005**, *39* (11), 4317–4320.
(10) Call, D.; Logan, B. E. Hydrogen production in a single chamber microbial electrolysis cell lacking a membrane. *Environ. Sci. Technol.* **2008**, *42* (9), 3401–3406.
(11) Cheng, S.; Liu, H.; Logan, B. E. Increased performance of single-chamber microbial fuel cells using an improved cathode structure. *Electrochem. Commun.* **2006**, *8* (3), 489–494.
(12) Lovley, D. R.; Phillips, E. J. Novel mode of microbial energy metabolism: organic carbon oxidation coupled to dissimilatory reduction of iron or manganese. *Appl. Environ. Microbiol.* **1988**, *54* (6), 1472–1480.
(13) Cheng, S. A.; Xing, D. F.; Call, D. F.; Logan, B. E. Direct biological conversion of electrical current into methane by electromethanogenesis. *Environ. Sci. Technol.* **2009**, *43* (10), 3953–3958.
(14) Selembo, P. A.; Merrill, M. D.; Logan, B. E. The use of stainless steel and nickel alloys as low-cost cathodes in microbial electrolysis cells. *J. Power Sources* **2009**, *190* (2), 271–278.
(15) APHA et al. *Standard methods for the examination of water and wastewater*, 18th ed.; American Public Health Association: Washington, DC, 1992.
(16) Veerman, J.; Post, J. W.; Saakes, M.; Metz, S. J.; Harmsen, G. J. Reducing power losses caused by ionic shortcut currents in reverse electrodialysis stacks by a validated model. *J. Membr. Sci.* **2008**, *310* (1−2), 418–430.
(17) Logan, B. E.; Call, D. F.; Cheng, S.; Hamelers, H. V. M.; Sleutels, T.; Jeremiasse, A. W.; Rozendal, R. A. Microbial electrolysis cells for high yield hydrogen gas production from organic matter. *Environ. Sci. Technol.* **2008**, *42* (23), 8630–8640.
(18) Kiely, P. D.; Rader, G.; Regan, J. M.; Logan, B. E. Long-term cathode performance and the microbial communities that develop in microbial fuel cells fed different fermentation end-products. *Bioresour. Technol.* **2011**, *102* (1), 361−366.
(19) Winker, S.; Woese, C. R. A definition of the domains Archaea, Bacteria and Eucarya in terms of small subunit ribosomal-RNA characteristics. *Syst. Appl. Microbiol.* **1991**, *14* (4), 305–310.
(20) Good, I. J. The population frequencies of species and the estimation of population parameters. *Biometrika* **1953**, *40* (3−4), 237–264.
(21) Hughes, J. B.; Hellmann, J. J.; Ricketts, T. H.; Bohannan, B. J. M. Counting the uncountable: Statistical approaches to estimating microbial diversity. *Appl. Environ. Microbiol.* **2001**, *67* (10), 4399–4406.
(22) Bianchi, M. A. G.; Armand, J. M. B. Statistical sampling of bacterial strains and its use in bacterial diversity measurement. *Microb. Ecol.* **1982**, *8* (1), 61–69.
(23) Kiely, P. D.; Call, D. F.; Yates, M. D.; Regan, J. M.; Logan, B. E. Anodic biofilms in microbial fuel cells harbor low numbers of higher-power-producing bacteria than abundant genera. *Appl. Microbiol. Biotechnol.* **2010**, *88* (1), 371−380.
(24) Kiely, P. D.; Cusick, R.; Call, D. F.; Selembo, P. A.; Regan, J. M.; Logan, B. E. Anode microbial communities produced by changing from microbial fuel cell to microbial electrolysis cell operation using two different wastewaters. *Bioresour. Technol.* **2011**, *102* (1), 388−394.
(25) Richter, H.; Lanthier, M.; Nevin, K. P.; Lovley, D. R. Lack of electricity production by Pelobacter carbinolicus indicates that the capacity for Fe(III) oxide reduction does not necessarily confer electron transfer ability to fuel cell anodes. *Appl. Environ. Microbiol.* **2007**, *73* (16), 5347–5353.
(26) Cheng, S.; Logan, B. E. Sustainable and efficient biohydrogen production via electrohydrogenesis. *Proc. Natl. Acad. Sci. U.S.A.* **2007**, *104* (47), 18871–18873.
(27) Tartakovsky, B.; Manuel, M. F.; Wang, H.; Guiot, S. R. High rate membrane-less microbial electrolysis cell for continuous hydrogen production. *Int. J. Hydrogen Energy* **2009**, *34* (2), 672–677.
(28) Rozendal, R. A.; Hamelers, H. V. M.; Molenkamp, R. J.; Buisman, C. J. N. Performance of single chamber biocatalyzed electrolysis with different types of ion exchange membranes. *Water Res.* **2007**, *41* (9), 1984–1994.
(29) Rozendal, R. A.; Sleutels, T. H.; Hamelers, H. V.; Buisman, C. J. Effect of the type of ion exchange membrane on performance, ion transport, and pH in biocatalyzed electrolysis of wastewater. *Water Sci. Technol.* **2008**, *57* (11), 1757–1762.
(30) Gordon, N. C.; Wareham, D. W. Multidrug-resistant Acinetobacter baumannii: mechanisms of virulence and resistance. *Int. J. Antimicrob. Agents* **2010**, *35* (3), 219–226.
(31) Martínez-Romero, E. Coevolution in Rhizobium-legume symbiosis. *DNA Cell Biol.* **2009**, *28* (8), 359–60.
(32) Logan, B. E. Exoelectrogenic bacteria that power microbial fuel cells. *Nat. Rev. Microbiol.* **2009**, *7* (5), 375–381.
(33) Caccavo, F.; Lonergan, D. J.; Lovley, D. R.; Davis, M.; Stolz, J. F.; McInerney, M. J. Geobacter sulfurreducens sp-nov, a hydrogen-oxidizing and acetate-oxidizing dissimilatory metal-reducing microorganism. *Appl. Environ. Microbiol.* **1994**, *60* (10), 3752–3759.
(34) Coppi, M. V.; Leang, C.; Sandler, S. J.; Lovley, D. R. Development of a genetic system for *Geobacter sulfurreducens*. *Appl. Environ. Microbiol.* **2001**, *67*, (7), 3180–3187.
(35) Badruzzaman, M.; Oppenheimer, J.; Adham, S.; Kumar, M. Innovative beneficial reuse of reverse osmosis concentrate using bipolar membrane electrodialysis and electrochlorination processes. *J. Membr. Sci.* **2009**, *326* (2), 392–399.
(36) Holmes, D. E.; Bond, D. R.; Lovley, D. R. Electron transfer by *Desulfobulbus propionicus* to Fe(III) and graphite electrodes. *Appl. Environ. Microbiol.* **2004**, *70* (2), 1234–1237.
(37) Bond, D. R.; Holmes, D. E.; Tender, L. M.; Lovley, D. R. Electrode-reducing microorganisms that harvest energy from marine sediments. *Science* **2002**, *295* (5554), 483–485.
(38) Tender, L. M.; Reimers, C. E.; Stecher, H. A.; Holmes, D. E.; Bond, D. R.; Lowy, D. A.; Pilobello, K.; Fertig, S. J.; Lovley, D. R. Harnessing microbially generated power on the seafloor. *Nat. Biotechnol.* **2002**, *20* (8), 821–825.

(39) Bond, D. R.; Lovley, D. R. Electricity production by *Geobacter sulfurreducens* attached to electrodes. *Appl. Environ. Microbiol.* **2003**, *69* (3), 1548–1555.
(40) Call, D. F.; Wagner, R. C.; Logan, B. E. Hydrogen production by *Geobacter* species and a mixed consortium in a microbial electrolysis cell. *Appl. Environ. Microbiol.* **2009**, *75* (24), 7579–7587.
(41) Rader, G. K.; Logan, B. E. Multi-electrode continuous flow microbial electrolysis cell for biogas production from acetate. *Int. J. Hydrogen Energy* **2010**, *35* (17), 8848−8854.
(42) Lee, H.-S.; Parameswaran, P.; Kato-Marcus, A.; Torres, C. I.; Rittmann, B. E. Evaluation of energy-conversion efficiencies in microbial fuel cells (MFCs) utilizing fermentable and non-fermentable substrates. *Water Res.* **2008**, *42* (6−7), 1501–1510.
(43) Chae, K.-J.; Choi, M.-J.; Kim, K.-Y.; Ajayi, F. F.; Park, W.; Kim, C.-W.; Kim, I. S. Methanogenesis control by employing various environmental stress conditions in two-chambered microbial fuel cells. *Bioresour. Technol.* **2010**, *101* (14), 5350–5357.

ES1025646